CrystEngComm

Accepted Manuscript

ROYAL SOCIETY OF CHEMISTRY

www.rsc.org/crystengcomm

A high temperature supramolecular-based switchable dielectric material with electrical bistability between high and low dielectric states

Cheng Chen[#], Fang-Fang Wang[#], Yi Zhang, Qiong Ye, Heng-Yun Ye, Da-Wei Fu*
(Ordered Matter Science Research Center, College of Chemistry and Chemical Engineering, Southeast University, Nanjing, 211189, P.R. China)

Abstract: One new hybrid supramolecular-based phase transition compound TAPC containing macrocycle stator with electrical bistability between high and low dielectric states (TAPC = $[(TAP\text{-}NH_3)\cdot(18\text{-crown-}6)\cdot 0.5(H_2O)]\cdot 2(ClO_4)$ **(1),** $TAP\text{-}NH_3$ = 4-ammonio-2,2,6,6-tetramethylpiperidinium**),** has been prepared and characterized by variable-temperature crystal structure determinations, elemental analysis, differential scanning calorimetry (DSC) and temperature-dependent dielectric spectroscopy. DSC measurement showed a pair of sharp peaks at 357 K (heating) and 322 K (cooling), indicating that TAPC undergoes a reversible first-order phase transition. The crystal structures determined at 293 K and 368 K are both monoclinic in the space group of $P2_1/m$. The most distinct difference between room-temperature and high-temperature structures is the order–disorder transition of the ClO_4^- anions and the displacement of the guest water molecules, which are the driving force of the high-temperature phase transition of electrical bistability (two incentives synergistically induced the phase transition). This functional moiety could be a cation/anion or guest molecule solely, observed in a lot of compounds, and very few of them belong to collaborative type (order-disorder motion and displacement) with the high temperature dielectric phase transitions. In addition, the large thermal hysteresis of 37.2 K contribute to a widely tunable transition between high and low dielectric states. Such distinctive dielectric performances suggest that **1** might be a potential high temperature switchable dielectric material.

Key Words: Phase transition; Electrical bistability; Supramolecular-based; Order–disorder

1. Introduction

Phase transition materials (PTMs) with electrical bistability have attracted great attention since they may be widely used in data communication, signal processing and rewriteable optical data storage, etc.[1] Searching for a new temperature-triggered solid-to-solid phase transition materials (SSPTMs) is very significant theoretically for the exploration and application of novel physical properties, the solid-to-solid phase change materials usually show an abrupt change of some physical properties around the transition temperature (Tc).[2] Recently, a series of researches have been conducted on solid-to-solid phase transitions in organic-inorganic hybrid complexes, which possess the properties and advantages of both organic and inorganic compounds, such as environment-friendly, flexible, easy to modify, free of heavy metals, etc.[3] In most reported cases, only one moiety in a compound has been able to display one-off freezing or ordering, resulting in one single phase transition. For instance, Zhang and luo et al. discovered a hybrid crystal exhibiting a tunable and switchable dielectric constant, which originated from an order–disorder phase transition, owing to the dynamical variation of the polar cation. And in these examples, most of them belong to the low temperature phase transition, the high temperature phase transitions are very scarce. This functional moiety could be a cation/anion or guest molecule solely, observed in a lot of compounds, and few of them belong to collaborative type with the high temperature dielectric phase transitions.[4] High-temperature dielectric material with electrical bistability between high and low dielectric states has a very wide range of applications.

Crown ethers are a kind of typical host molecules of organic-inorganic hybrid complexes, the protonated R-NH_3^+ cation (R = aryl or alkyl ring) is easily anchored in the cavity of 18-crown-6, which is a good molecular stator or pendulator in molecular machine design. As a continuation of our study on phase transition materials including crown ethers,[5] we reported our working here on the 1:1 complexes of 18-crown-6 with 4-Amino-2,2,6,6-tetramethylpiperidine perchlorate, which shows obvious switchable dielectric electrical bistability at room-temperature and high-temperature,

respectively. Generally, the 18-crown-6 molecule acts as a host of which the six O atoms afford lone-pair electrons to anchor the guest $R–NH_3^+$ cation or H_2O molecule. The guest molecules may undergo rotational or local wobbling/twisting motion, producing an order–disorder type transition. An example of phase transition triggered by the motion of guest molecule has been observed in our previous work ($[(C_7H_7O\text{-}NH_3)(18\text{-crown-}6)]\cdot[AB_4^-]$),[6] in which order–disorder transition of the pendulum-like motions of the terminal para-methyl group of the 4-methoxyanilinium guest cation resulted in a ferroelectric-paraelectric phase transition with electrical bistability. As a continuity of our work, the new host–guest compound $[(TAP\text{-}NH_3)\cdot(18\text{-crown-}6)\cdot 0.5(H_2O)]\cdot 2(ClO_4)$, which is analogous to $[(C_7H_7O\text{-}NH_3)(18\text{-crown-}6)]\cdot[BF_4^-]$ structurally,[7] also shows the phase transition behavior. It is found not from motional changes of the $TAP\text{-}NH_3^{2+}$ guest cation, however, the most distinct difference between room-temperature and high-temperature structures is the order–disorder transition of the ClO_4^- anion and the displacement of the guest water molecule, which are the driving force of the high-temperature phase transition of electrical bistability between high and low dielectric states (two incentive synergistically induced the phase transition).

2. Experimental section

2.1 Preparation of crystal 1. All chemical reagents were used without further purication. Compound **1** was synthesized through reaction of 4-amino-2,2,6,6-tetramethylpiperidine, $HClO_4$ and 18-crown-6 with a 1:2:1 molar ratio. The 4-amino-2,2,6,6-tetramethylpiperidine (1.56 g, 0.01mol) was dissolved into 30 mL of distilled water and then the 2.86 g(0.02 mol) perchloric acid was added; finally the 18-crown-6 (2.64 g, 0.01 mol) was added with stirring and heating. The synthesized solution was kept at room temperature and colorless block crystals were obtained by slow evaporation from the aqueous solution after several days.

2.2 Single-crystal X-ray crystallography. X-Ray diffraction experiment was carried out using a Rigaku Saturn 724 diffractometer with Mo-Ka radiation (λ=0.71073Å). Data processing including empirical absorption correction was performed using the

crystalclear software package (Rigaku, 2005). The structure was solved using direct methods and successive Fourier difference synthesis (SHELXS-2014), and refined using the full-matrix least-squares method on F^2 using the SHELXTL software package. Non-H atoms were refined anisotropically using all reflections with I > 2s(I). H atoms on C atoms were placed in calculated positions and refined using 'riding' model and ammonium H atoms were obtained from the Q peaks in difference Fourier maps. Crystallographic data and details of the data collection and refinement are summarized in Table 1.

Table 1. Summary of crystallographic data for compound **1** at 293K and 368K

	RTP(293K)	HTP(368K)
Empirical formula	$C_{21}H_{46}Cl_2N_2O_{14.5}$	$C_{21}H_{46}Cl_2N_2O_{14.5}$
Formula weight	629.50	629.50
Crystal system Space group	Monoclinic $P2_1/m$	Monoclinic $P2_1/m$
Temperature(K)	293	368
a (Å)	10.337(2)	10.432(13)
b (Å)	11.655(2)	11.734(14)
c (Å)	13.504(3)	13.639(16)
β (º)	108.17(3)	108.53(2)
Volume (Å^3)	1545.8(5)	1583(3)
Radiation type	Mo-Kα	Mo-Kα
Absorption correction	Multi-scan	Multi-scan
Z, Calculated density	2, 1.351 Mg/m^3	2, 1.321 Mg/m^3
F(000)	671.0	672.0
Tmin/max	0.910/1.000	0.910/1.000
GOF	1.117	1.049
R1 [I>2s(I)]	0.0916	0.0891
wR2 [I>2s(I)]	0.2373	0.2164

2.3 Dielectric properties and DSC measurement. The temperature dependence of the dielectric constant was measured using a Tonghui TH2828A impedance analyzer in the temperature range of 300−380 K at the frequency of 1 MHz with the measuring AC voltage fixed at 1 V. The electrodes were made by sputtering silver onto both sides of samples and attaching copper leads with silver paste. The DSC measurement was performed on NETZCSCH DSC 200 F3 instrument by heating and cooling rate of 2 K/min in the temperature range of 300−400 K.

2.4 IR spectrum , powder X-ray diffraction and TG measurement. The IR spectrum of **1** shows a strong vibration peak between 1150 and 1100 cm^{-1}, indicative of the existence of perchlorate anion (see supplementary material, Fig. S1). The powder X-ray diffraction (PXRD) pattern of **1** at room temperature matches very well

with the pattern simulated from the single crystal structure (see supplementary material, Fig. S2). TG experiment started with an increasing heating rate of 10 °C /min(from 50 °C to 500 °C), It should be remarked that no significant weight loss was observed until 110 °C. (see supplementary material, Fig. S3).

3. Results and Discussion

The details of the structural phase transition of compound **1** were revealed by the determination of variable-temperature crystal structures at 293 K (the room temperature phase, RTP) and 368K (the high temperature phase, HTP), respectively (Fig.1).For both RTP and HTP, the complex is crystallized in the monoclinic system with $P2_1/m$ space group. An asymmetry unit for the complex [(TAP-NH3)•(18-crown-6)•0.5(H2O)]•2(ClO4) consists of half TAP-NH_3^{2+} cations, half 18-crown-6 molecular, a quarter water molecular and two half ClO_4^- anions. In order to further investigate the structural changes, the RTP and HTP structures are compared in detail (see supplementary material, Table. S1 and S2).

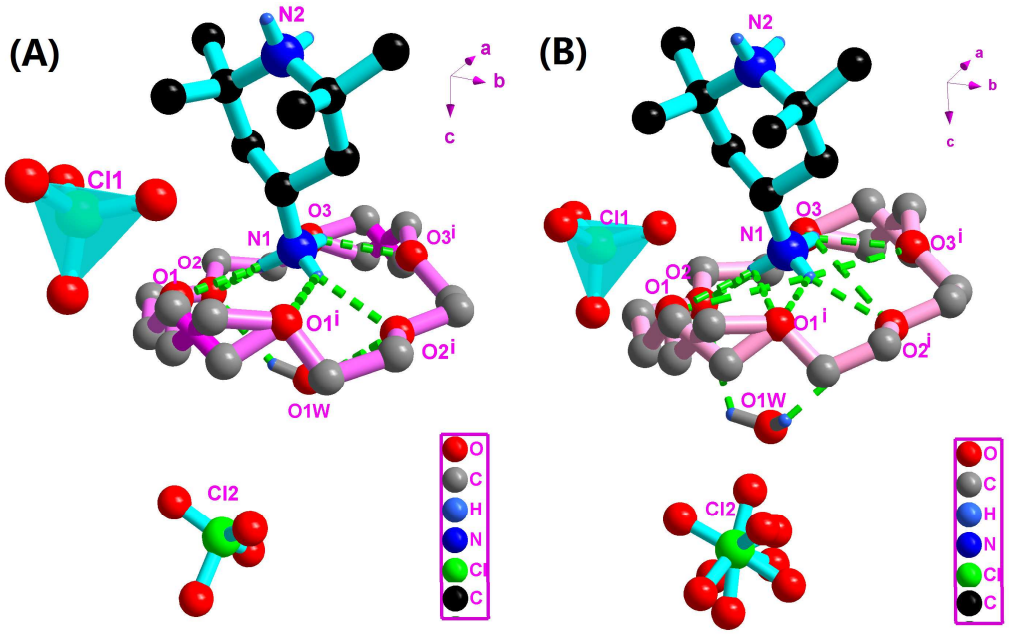

Fig. 1 The asymmetric unit of **1** was shown at different temperatures. (A) The room temperature phase (293 K): the ClO_4^- anion is totally ordered and the H_2O molecular lies just below the center of crown ether. (B) The high temperature phase (368 K): One of the ClO_4^- anion is totally disordered and the H_2O molecular lies

bottom left of the crown ether. Carbon-bound H atoms were omitted for clarity and the intramolecular N-H···O hydrogen bonds are shown as dashed lines (symmetry code: (i) x,1/2- y,1+z).

In the room temperature (RTP) structure, The $–NH_3^+$ locates in the 18-crown-6 ring to form a supramolecular rotator-stator-like structure by intermolecular N-H···O interactions between the $–NH_3^+$ and $O_{18\text{-crown-6}}$ atoms (Fig. 1A). The strong N-H···O interactions fall within the normal range of 2.883(7)–2.952(5) Å and the N-H···O bond angles of 129.5–150.8°, indicating dipolar donor–accepter attractions. One H_2O molecular lies just below the center of crown ether ring with weaker O-H···O interactions fall within the normal bond distances of 3.10(2) Å and the O-H···O bond angles of 150.7°, hydrogen bonding interaction between H_2O and two O atoms may contribution to six O atoms of crown ether located on different plane. The four oxygen atoms on the crown ether lie approximately in a same plane, another two oxygen atoms below this plane. The two ClO_4^- anions are presented as counter ion to the supramolecular $[(TAP\text{-}NH_3)\cdot(18\text{-crown-6})]^{2+}$ cation, one adopts a nearly ideally tetrahedral geometry with the O-Cl bond distances of 1.399(4)–1.425(6) Å and the O-Cl1-O bond angles of 108.6(5)–110.1(5)°, another one present a twisty tetrahedral geometry with the O-Cl bond distances of 1.194(15)–1.361(15) Å and the O-Cl2-O bond angles of 97.4(16)–118.6(9)°. Besides, there exist no classical hydrogen bonds are found between the ClO_4^- tetrahedra and $[(TAP\text{-}NH_3)\cdot(18\text{-crown-6})]^{2+}$ moiety.

In the high temperature (HTP), both one of two ClO_4^- anion and the H_2O molecular changed obviously compared with that in RTP, and the order–disorder transition was occurred for the ClO_4^- anion with four O atoms spliting into nine, with the abnormal O-Cl bond distance fall within range of 1.271(4)-1.508(9) and the O-Cl2-O bond angles of 36.8(7)-178.2(4). The occupancies assigned to O atoms were changed at the last stage of refinement to keep the ratio of O to Cl (2:0.5 or 4:1). If the occupancies assigned to O atoms were not changed, then the total number of O atoms will be more than 4. Therefore, according to the Ueq the occupancies were altered accordingly. The H_2O molecule lie in the bottom left of the crown ether with weaker O-H···O interactions fall within the bond distances of 3.591(14) Å. While another

ClO_4^- adopts a nearly ideally tetrahedral geometry with the O-Cl1 bond distance of 1.409 (2)-1.430(3) Å and the O-Cl1-O bond angles of 108.82(13)–109.89(10)°. The $–NH_3^+$ nests in the 18-crown-6 ring to form a supramolecular rotator-stator-like structure by intramolecular N-H···O interactions between the $–NH_3^+$ and six oxygen atoms [O1, O2, O3, $O1^i$, $O2^i$ and $O3^i$ symmetry code i for (x, 1/2−y, 1+z)] on the crown ether. The strong N-H···O interactions fall within the normal range of 2.902(3)–2.971(3) Å and the N-H···O bond angles of 130.2–150.5°, indicating dipolar donor–accepter attractions. The conformation of the crown-ether ring and the hydrogen-bond geometry in the assemblies closely resemble those in related adducts of 18-crown-6 and primary alkylammonium salts.[8]

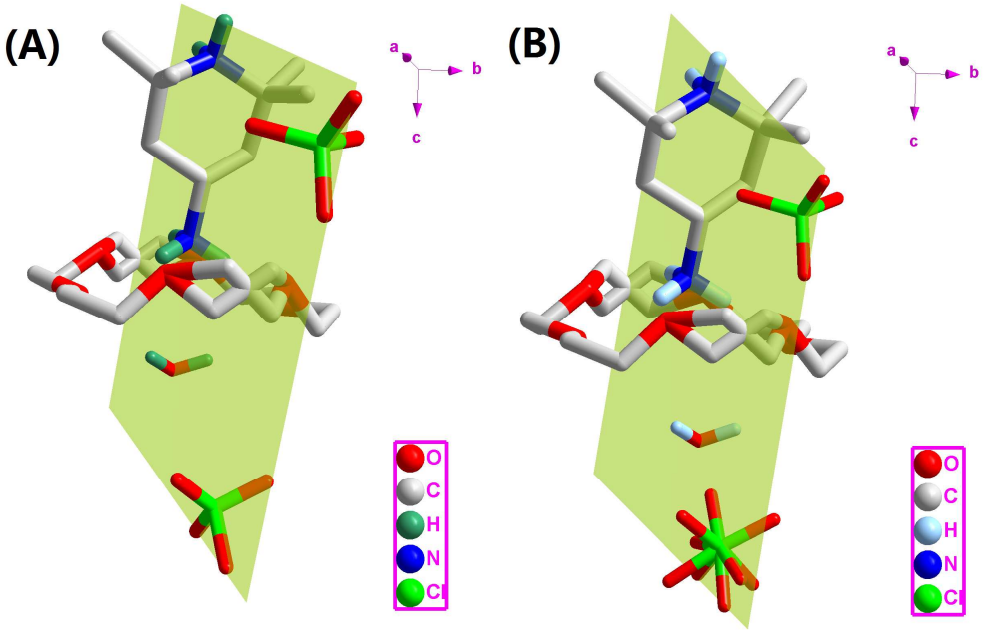

Fig. 2 Mirror plane for the asymmetric unit of **1** in the RTP(A) and HTP(B)

In the asymmetric unit of the RTP and HTP structure, the 13 non-hydrogen atoms (C15, N1, N2, O9, O10, O11, O12, O14, O16, O17, O1W, Cl1 and Cl2) located on a mirror plane, other non-H atoms apart from the above mirror plane can be produced by a (x, 1/2−y, 1+z) symmetry transformation. The TAP-NH_3^{2+} moiety nests almost perpendicularly in the crown ring with an angle of 88.2°. Interestingly the five O atoms of one disorder ClO_4^- anions are just on the mirror plane, and above Tc=357 K these atoms swings around the two sides of the mirror plane with the same

probability (Fig. 2).

One of the two notable differences between the HTP and RTP structures is the relative displacement of H_2O molecule guest (Fig. 3A, and Fig.3B), and the relative displacement will be one of the driving forces of the phase transition. When viewed down the *b*-axis (Fig.3B), it is clear that the relative displacement along the *a*-axis is rather large on the crystallography mirror plane. The distance is ca.1.3803 Å away from central axis of 18-crown-6 ring in the HTP structure, however, the position of water molecule is overlapped with the central axis of 18-crown-6 ring in the RTP structure.

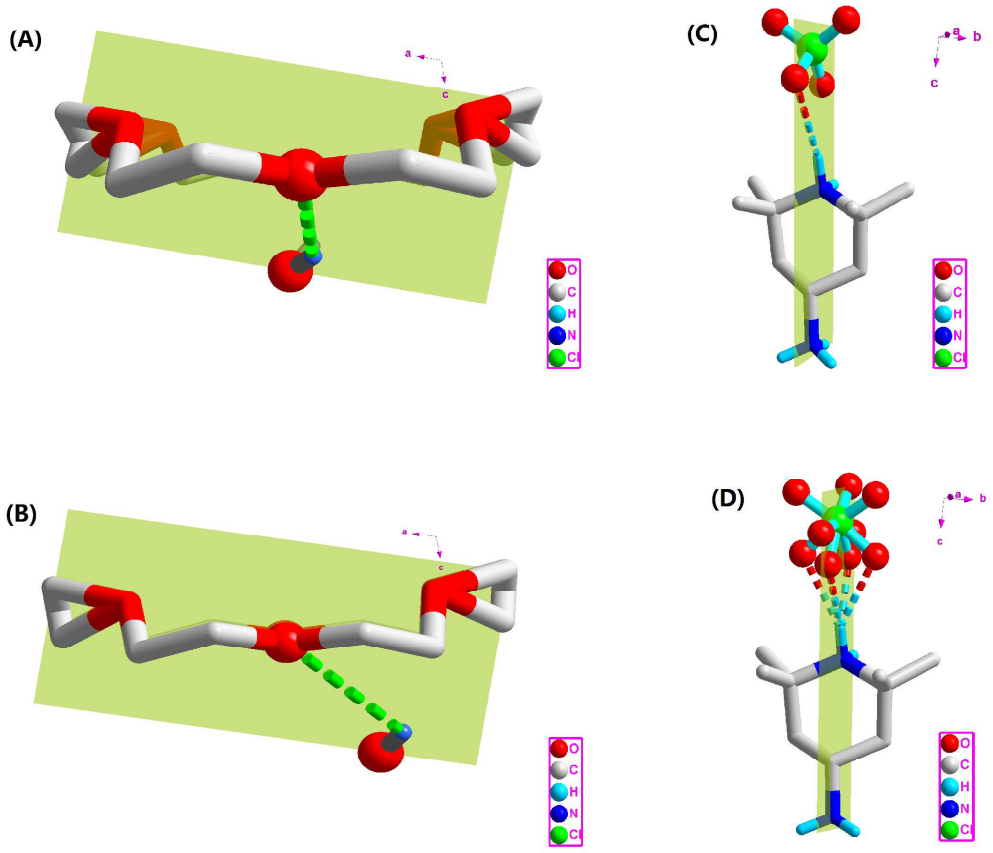

Fig. 3 Obvious displacement of H_2O molecule: (A) RTP and (B) HTP structure; Order-disorder transition of ClO_4^- and the hydrogen bond between the TAP-NH_3^{2+} cation and ClO_4^- anion along the *c*-axis: (C) RTP and (D) HTP structure

For the structures of the hydrogen-bonded chains in the HTP and RTP, the another one notable difference is the hydrogen-bond interactions between the

TAP-NH_3^{2+} cation and one of two ClO_4^- anions along the *c*-axis. As checked by PLATON (Spek,2003), the orientation of the major parts of the ClO_4^- anions is conducive to the formation of hydrogen bonds to the TAP-NH_3^{2+} cations. Fig.4D shows a diagram of hydrogen-bonding interactions between the disordered anion and the cations at HTP. For the ClO_4^- anion, there are four disordered O atoms are linked to the H atoms by hydrogen bonds, while in the RTP structure there is only one O atom of perchlorate is linked to the TAP-NH_3^{2+} cations. Thus, the hydrogen-bond interactions strength between the RTP and HTP has been changed. Therefore, the order-disorder transition of ClO_4^- is one of the driving forces of the phase transition.

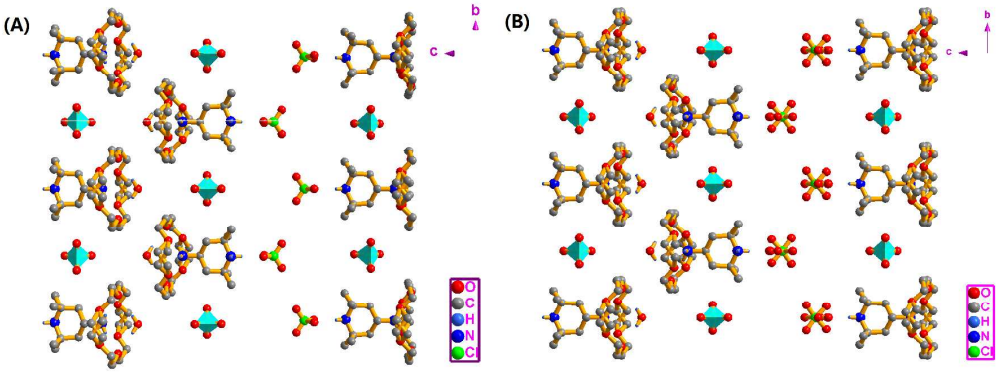

Fig. 4 Packing diagrams view along the *a*-axis, A for RTP and B for HTP structure.

As shown in Table 1, the room temperature phase (RTP) and high temperature phase (HTP) structures located in the same monoclinic $P2_1/m$ space group, and the cell parameters showed no obvious differences in the two phases. This suggests that the driving force of the phase transition is not enough to change the spatial symmetry. Furthermore, from the packing views along with the *c*-axis, the packing diagrams in the HTP and RTP looks similar except the order-disorder transition of ClO_4^- and displacement of guest water molecule, no other obvious change contributing to the phase transition (Fig. 4).

One of the best ways to detect whether a compound displays phase transitions triggered by temperature is to perform DSC measurement to confirm the existence of a heat anomaly occurring during the heating and cooling process. Therefore, the DSC measurement of compound **1** exhibited highly remarkable reversible structural phase transition (Fig. 5). Upon heating and cooling course, the sample of **1** undergoes a

distinguished phase transition by showing a large endothermic peak at 357.5 K and an exothermic peak at 322.3 K. These observed peaks represent a prominent and reversible phase transition with a large thermal hysteresis of 37.2K. Both the sharp shape of the peaks and the thermal hysteresis reveal the discontinuous character of the transition, being effectively indicated the presence of a first-order phase transition. Entropy change ΔS accompanying the phase transition was estimated as≈3.41J mol^{-1} K^{-1}. Given that ΔS = nRlnN, where R is the gas constant and N is the ratio of possible configurations in the disorder system, it obtains N = 1.51, indicating that an extremely complex transition other than a typical order–disorder transition undergoing reorientations at two sites (N = 2) takes place. As for the origin of the asymmetry of exothermic peak and endothermic peak, it may attribute to the double structure changes of order-disorder of ClO_4^- anion and displacement of water molecule, which requires in-depth study. TG measurement shows that the loss of H_2O occurred at 400K, the value is in accordance with the calculated value for the loss of $1/2H_2O$ per formula (ca.1.509%) (see supplementary material, Fig. S3), these result prove the stability of H_2O molecule in phase transition temperature ranges (320-360K), finally indicating the electrical bistability of the phase transition on both heating and cooling stages. In addition, eminent dielectric anomalies observed at ca.350 K (heating) and ca.325 K (cooling) further confirm the presence of phase transition (Fig.6). Large-size crystals were successfully grown from the ethanol-water solutions as the plates perpendicular by the temperature programmed cooling methods (Fig.5B).

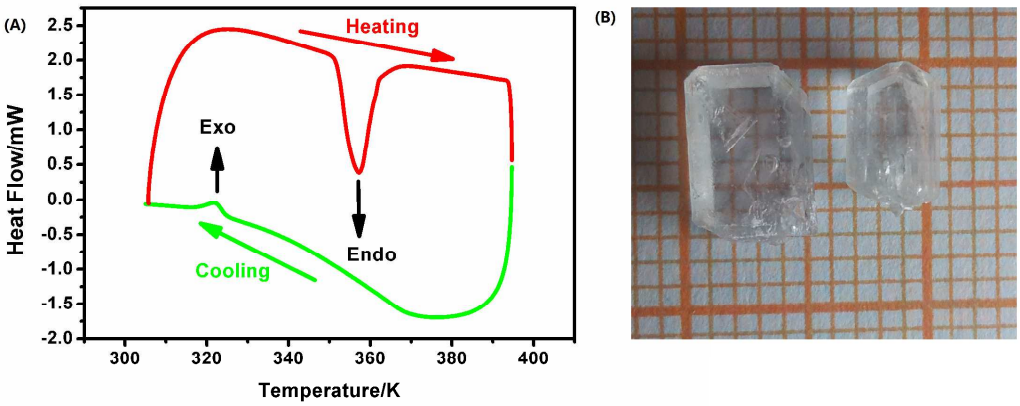

Fig.5 (A) DSC measurements obtained on a heating-cooling cycle of compound **1**

(B) The as-grown crystals of **1** with the respective sizes of 7.2 ×5.2 × 4.3 mm^3 and 6.1× 3.4 × 2.6 mm^3 .

As we all known that the phase transition will be accompanied by anomaly of physical properties near the structure phase transition point, such as the dielectric constant (both real part and imaginary part) which we used for looking for new phase transition materials and detecting phase transition point under different frequencies.[9] The single crystal sample of **1** was applied to the dielectric measurements with the measurement temperature range of 300−380 K. As expected, the results distinctly reveal that the real part demonstrates a step-like change both at heating (Tc = 357 K) and cooling process with the thermal hysteresis of 25 K (Fig. 6 A), which is treated as the extremely effective indicator of the structural phase transition, corresponding well with the phase transition temperature determined by DSC. The real and imaginary parts of the dielectric permittivity ($\varepsilon = \varepsilon' + i\varepsilon''$) always exhibit a very strong temperature dependence, particularly, the dielectric permittivities is very high in HTP, while in RTP become lower into a different magnitude. As for details, the real part of dielectric constant ε' at 5 kHz remains at approximately 7.5 below Tc=357 K and displays a significant change up to about 11.5, that is to say, the dielectric permittivity shows an obvious augment followed by a distinct slope, subsequently exhibits a plateau with a slight aggrandizement. Such dielectric behaviors with the change of temperature are very consistent with the characteristic of switchable molecular dielectric.[10] Corresponding with the dielectric constant (ε'), the imaginary part, measured at fixed frequencies of 5 kHz, 10 kHz, 100 kHz and 1 MHz, also exhibited a clear step-like change and showed a significant dielectric relaxation process at different frequencies upon heating process (Fig. 6B), which effectively confirmed the presence of phase transition between 320K and 360K.[11] As shown in Fig. 6B, with the decrease of the frequency, the temperature of the peak maximum of the imaginary parts (ε'') moves progressively towards lower temperatures, and the peak amplitudes increase distinctively. This phenomenon is well in line with what happened in classical dielectric relaxors accompanied by the prominent dielectric anomaly during the structural phase transition. The origin of the phase transition was

ascribed to both the order–disorder transition of perchlorate anion and the displacement of guest water molecule, which are the driving force of the high-temperature phase transition with electrical bistability (two incentives synergistically induced the phase transition). Very few of PCMs belong to collaborative type with the high temperature dielectric phase transitions. High-temperature dielectric material with electrical bistability between high and low dielectric states has a very wide range of applications. As a new supramolecular PCMs, we believe that these findings will open a new avenue for the design of smart materials.

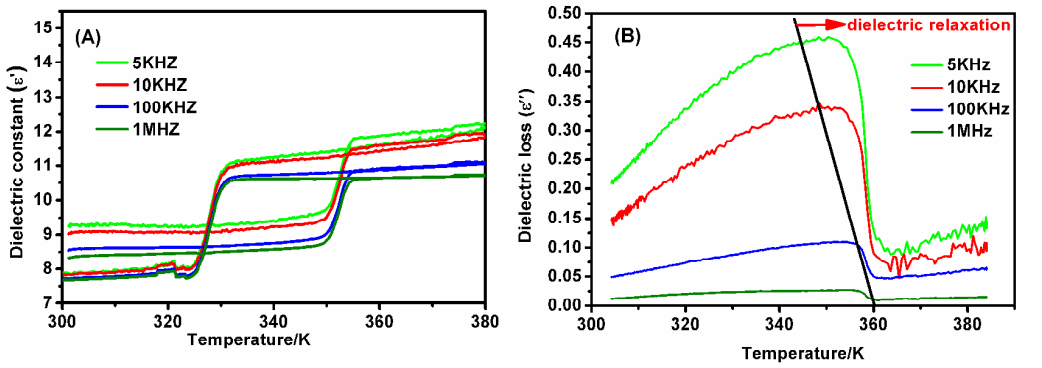

Fig. 6 (A) Temperature dependence of dielectric constants of compound **1**, (B) The dielectric loss as the function of temperature was measured at fixed frequencies of 5 kHz, 10 kHz, 100 kHz and 1 MHz are presented upon the heating process.

4.Conclusion

In summary, we have presented a new host-guest compound, which undergoes a reversible phase transition at ca.357 K make it a potential switchable dielectric material with electrical bistability. DSC measurement reveals that the phase transition occurs between 320-360 K. And the dielectric anomalies were observed at 350 K (heating) and 325 K (cooling) further confirmed the bistable phase transition. The origin of the phase transition was ascribed to both the order–disorder transition of perchlorate anion and the displacement of guest water molecule, which are the driving force of the high-temperature phase transition with electrical bistability (two incentives synergistically induced the phase transition). Very few of PCMs belong to

collaborative type with the high temperature dielectric phase transitions. High-temperature dielectric material with electrical bistability between high and low dielectric states has a very wide range of applications. As a new supramolecular PCMs, we believe that these findings will open a new avenue for the design of smart materials.

Acknowledgments

This work was financially supported by the Project 973 (2014CB848800), National Natural Science Foundation of China (21422101, 21301029), Jiangsu Province NSF (BK20130600, BK20140056), Program for NCET and Ph.D. Programs Foundation of Ministry of Education of China (20130092120013). #These authors contributed equally to this work. Also we gratefully thank Prof.Ren-Gen Xiong for revising this manuscript.

Appendix A. Supplementary data

Supplementary material related to this article can be found, in the online version, at ??. CCDC-1025179 (293K) and 1025180 (368K) contain the supplementary crystallographic data for this paper. This data can be obtained free of charge from the Cambridge Crystallographic Data Centre via www.ccdc.cam.ac.uk/data_request/cif.

References

1 (a) D. W. Fu, H. L. Cai, Y. Liu, Q. Ye, W. Zhang, Y. Zhang, X. Y. Chen, G. Giovannetti, M. Capone, J. Y. Li, R. G. Xiong, Science, 2013, 339 ,425-428; (b) Z. Czapla, S. Dacko, A. Waskowska, J. Phys. Condens. Matter, 2003, 15, 3793-3803; (c) S. Horiuchi, R. Kumai, Y. Okimoto, Y. Tokura, Chem. Phys., 2006, 325 ,78-91; (d) R. Jakubas, G. Bator, M. Gosniowska, Z. Ciunik, J. Baran, J. Lefebvre, J. Phys. Chem. Solids, 1997, 58 , 989-998.

2 (a) W. P. Li, D .S. Zhang, T. P. Zhang, T. Z. Wang, D .S. Ruan, D. Q. Xing, H. B. Li, Thermochim. Acta, 1999, 326, 183-186; (b) H. Y. Ye, L. Z. Chen, R. G. Xiong, Acta Crystallogr., 2010, 66, 387-395; (c) K. Prout, S. J. Heyes, C. M. Dobson, A. McDaid, T. Maris, M. Muller, M. Seaman, J. Chem. Mater., 2000, 12, 3561-3569; (d) W. Gao, L. Dickinson, C. Grozinger, F. G. Morin, L. Reven, Langmuir, 1997, 13, 115-118.

3 (a) W. Zhang, H. Y. Ye, H. L. Cai, J. Z. Ge, R. G. Xiong, S. D. Huang, J. Am. Chem. Soc., 2010, 132, 7300-7302; (b) H. Y. Ye, J. Z. Ge, F. Chen, R. G. Xiong, CrystEngComm, 2010, 12, 1705-1708; (c) W. Zhang, Y. Cai, R. G. Xiong, H. Yoshikawa, K. Awaga, Angew. Chem. Int. Ed., 2010, 49, 6608-6610.

4. (a) D. W. Fu,W. Zhang, H. L. Cai, J. Z. Ge, Y. Zhang, R. G. Xiong, Adv. Mater.,

2011,23,5658-5662; (b) P. Zhou, Z. H. Sun, S. Q. Zhang, C. M. Ji, S. G. Zhao, R. G. Xiong, J. H. Luo, J. Mater. Chem. C, 2014, 2, 2341–2345

5 (a) D. W. Fu; H. L. Cai; S. H. Li; Phys. Rev. Lett., 2013, 110, 257601; (b) Y. Zhang, H. Y. Ye, D. W. Fu, R. G. Xiong, Angew. Chem. Int. Ed., 2014, 53, 5064-5068; (c) H. Y. Ye, Y. Zhang, D. W. Fu, R. G. Xiong, Angew. Chem. Int. Ed., 2014, 53, 6724-6729; (d) H. Y. Ye, S. H. Li, Y. Zhang, L. Zhou, F. Deng, R. G. Xiong, J. Am. Chem. Soc., 2014, 136, 10033-10040.

6 (a) H. L. Cai; D. W. Fu; Y. Zhang; Phys. Rev. Lett., 2012, 105, 169601. (b) H. Y. Ye, H. L. Cai, J. Z. Ge, R. G. Xiong, J. Appl. Crystallogr., 2010, 43, 1031-1035;(c) H. L. Cai, W. Zhang, J. Z. Ge, Y. Zhang, K. Awaga, T. Nakamura, R. G. Xiong, Phys. Rev. Lett., 2011, 14, 147601-147604; (d) W. Zhang, Y. Cai, R.G. Xiong, H. Yoshikawa, K. Awaga, Angew. Chem. Int. Ed., 2010,49,6608-6610.

7 (a) D. W. Fu, W. Zhang, H. L. Cai, Y. Zhang, J. Z. Ge, R. G. Xiong, S.D. Huang, J. Am. Chem. Soc., 2011, 32, 12780-12786; (b) D. E. O'Reilly, E. M. Peterson, D. L.Hogenboom, J. Chem. Phys., 1972, 57, 3969-3976; (c) Q. Ye, T. Akutagawa, H.-Y. Ye, T. Hang, J. Z. Ge, R. G. Xiong, S. i. Noro, T. Nakamura, CrystEngComm, 2011, 13, 6185-6191.

8 (a) D. Henschel, A. Blaschette, P. G. Jones, Acta Crystallogr., 1997, 53, 1875-1877; (b) Bandy, J. A, Truter, M. R. Wingfield, J. N. Lamb, J. D. J. Chem. SOC, Perkin Trans., 1981, 2, 1025-1030.

9 (a) Y. Zhang, K. Awaga, H. Yoshikawa, R.G. Xiong, J. Mater. Chem., 2012, 22, 9841-9845; (b) S. Horiuchi, R. Kumai, Y. Okimoto, J. Am. Chem. Soc., 1999, 121, 6757-6758; (c) H. X. Zhao, X. J. Kong, H. Li, Y. C. Jin, L. S. Long, X. C. Zeng, R. B. Huang, L. S. Zheng, Proc. Natl. Acad. Sci. U. S. A., 2011, 108, 3483-3486; (d) Z. H. Sun, T. L. Chen, J. H. Luo, M. C. Hong, Angew. Chem., Int. Ed, 2012, 51, 3871-3876.

10 (a) X. J. Shi, J. H. Luo, Z. H. Sun, S. G. Li, C. M. Ji, L. Li, L. Han, S. Q. Zhang, D. Q. Yuan, M. C. Hong, Cryst. Growth Des., 2013, 13, 2081-2086. (b) Z. Dominguez, T. A. Khuong, H. Dang, C. N. Sanrame, J. E. Nuñez, M. A. Garcia-Garibay, J. Am. Chem. Soc., 2003, 125, 8827-8837.

11 (a) G. Xu, Y. Li, W. W. Zhou, G. J. Wang, X. F. Long, L. Z. Cai, M. S. Wang, G. C. Guo, J. S. Huang, G. Batorb, R. Jakubas, J. Mater. Chem., 2009, 19, 2179-2183. (b) Z. H. Sun, J. H. Luo, T. L. Chen, L. Li, R. G. Xiong, M. L. Tong, M. C. Hong, Adv. Funct. Mater., 2012, 22, 4855-4861.

A high temperature supramolecular-based switchable dielectric material with electrical bistability between high and low dielectric states

Cheng Chen, Fang-Fang Wang, Yi Zhang, Qiong Ye, Heng-Yun Ye, Da-Wei Fu